Journal of Alloys and Compounds 527 (2012) 10–15

Contents lists available at SciVerse ScienceDirect

Journal of Alloys and Compounds

journal homepage: www.elsevier.com/locate/jallcom

Infiltration characteristics of liquid AZ91D alloy into short carbon fiber preform

L.H. Qi[a,*], L.Z. Su[a], J.M. Zhou[a], J.T. Guan[a], X.H. Hou[b], H.J. Li[c]

[a] School of Mechatronic Engineering, Northwestern Polytechnical University, Xi'an 710072, China
[b] Department of Mechanical, Materials, and Manufacturing Engineering, The University of Nottingham, University Park, Nottingham NG7 2RD, United Kingdom
[c] School of Materials Science and Engineering, Northwestern Polytechnical University, Xi'an 710072, China

ARTICLE INFO

Article history:
Received 29 September 2011
Received in revised form 21 February 2012
Accepted 24 February 2012
Available online xxx

Keywords:
Metal-matrix composites
Liquid–solid reactions
Liquid metal infiltration
Thermodynamic modeling

ABSTRACT

The infiltration characteristics of liquid AZ91D alloy into carbon fiber preform were investigated through a measuring device. The infiltration processes were monitored continuously using the thermocouples and electrical proportional valve. Experimental data were analyzed to establish the infiltration kinetics model and threshold pressure model, in which the uncertainties in the model about the fractal characters of porous media have been determined. The theoretical models and experiment data are compared and well matched. Results for the infiltration kinetics and threshold pressure were discussed also. The threshold pressure was found to be proportional to the volume fraction of fibers in the preform. And the control methods to improve the quality of the infiltration were also discussed.

1. Introduction

Due to the excellent mechanical and physical properties, C_{sf}/Mg composites are currently attracting much more attention from researchers [1,2]. In recent years, a number of techniques were developed which include powder metallurgy and the spray deposition and so on [3,4]. Liquid metal infiltration process is one of efficient methods for fabricating C_{sf}/Mg composites due to their significant potential at low costs [5]. Previous work on the infiltration has been conducted thoroughly on process and process modeling. Specific process routine was developed based on the liquid metal infiltration to apply external pressure to overcome the pressure differential due to capillary at the infiltration front [6], such as squeeze casting [7,8], gas pressure infiltration [9], vacuum infiltration [10,11], and extrusion directly following vacuum infiltration technique (EFVI) [12,13]. A more quantitative understanding of the infiltration behavior would enable better selection of infiltration materials, surface preparation, and processing parameters so that processing practice may be optimized [14]. For different liquid infiltration process, much research work had also been conducted on the calculation of the threshold pressure for initiation of infiltration [15,16], modeling of the infiltration processes [17,18], flow behavior of melt in the fiber preform [19,20] and multiscale simulation of unsaturated flows [21]. However, these theoretical results are different for different experimental conditions and also do not match with experimental results quantitatively. The suitable process models are required to investigate the infiltration behavior of melt magnesium into short carbon preform.

Additionally, the infiltration model is usually built by determining the relationship between the infiltration depth and the infiltration time. Due to the difficulties presented by the high temperature and high pressure applied during liquid infiltration processes for metal matrix composites (MMCs) fabrication, it is hard to investigate the flow behavior of molten alloy in the fiber preform by conventional techniques used in hydrodynamic research in porous media [22]. Concurrently three methods were reported to determine the infiltration depth in the literature. The infiltration depth can be measured with a precision gauge from the sectioned samples taken out of the melt [23]. In this method, series of experiments under different pressure need to be conducted in which the position of infiltration front can be obtained to relate the infiltration front with process parameters. The second method is that the infiltration depth can be indicated by pre-placed thermocouples in the preform through their rapid thermal response to the variation of ambient temperature, which was used to monitor the flow behavior of liquid alloy in the preform [15]. Another method used by Mortensen et al. [24] is that a sensor was developed to measure the position of the liquid metal in the fibrous preform during the infiltration process. SiC filament and molten metal were used as a variable resistor, and the liquid metal front could be calculated in order to change in the resistance of the sensor. These methods were suitable to investigate the flow behavior in fabricating aluminum matrix composites. Due to the complexity of infiltrating magnesium into carbon fiber preform caused by the inflammable property of liquid magnesium, gas protection device should be considered in experiments. The flow behavior of molten magnesium into the

* Corresponding author.
E-mail address: qilehua@nwpu.edu.cn (L.H. Qi).

0925-8388/$ – see front matter.
doi:10.1016/j.jallcom.2012.02.133

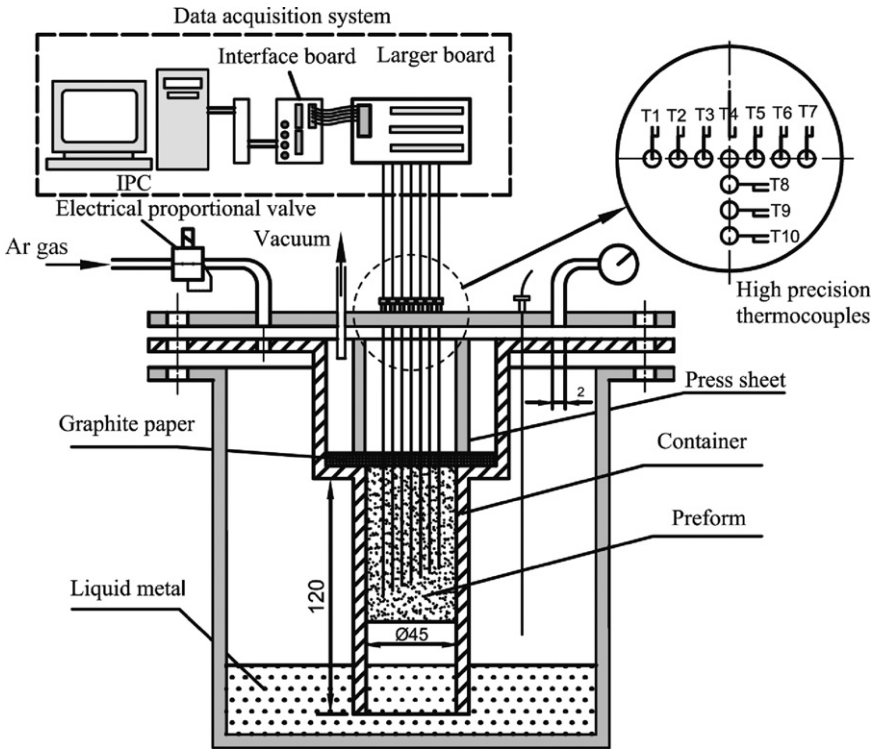

Fig. 1. Illustration of the experimental facility and thermocouple locations.

preform has not been investigated through the mentioned methods. So it is necessary to develop a realistic mathematical model to describe the infiltration characteristics of liquid magnesium alloy into a chopped short carbon fibrous preform. On the other hand, new experimental device also need to be developed to infiltrate magnesium into carbon preform which can monitor the evolution of infiltration depth changing with the time.

In this paper, mainly based on the second method abovementioned, a measuring device of vacuum assistant pressure infiltration was developed to investigate the infiltration characteristics of liquid AZ91D alloy into carbon fiber preform, which can monitor the dynamic infiltration process. At the same time, infiltration models were introduced to calculate the infiltration velocity and threshold pressure of infiltration process. The effects of fiber volume fraction of preform and infiltration pressure on the inflow velocity of molten metal were examined and discussed theoretically. The theoretical model was verified through infiltration experiments by use of the new developed infiltration experimental device.

2. Experimental and materials procedures

2.1. Materials

The main properties of the short carbon fiber used in this work are given in Table 1. The preform was prepared by wetting method in three steps. Firstly, carbon fibers were immersed into acetone to remove the organic binder and then were stirred in 0.5% aqueous sodium polyacyrlate solution for dispersing the fibers. Secondly, the carbon fiber slurry was poured into a mold to be shaped into the cylindrical preform of 25 mm in height and 45 mm in diameter which was later dried at room temperature for 24 h. The dried preform was baked at 120 °C in electronic furnace for 2–4 h. Thirdly, the baked preform was put into an isothermal chemical vapor infiltration furnace to be sintered at 1600 °C for several hours. More experimental details can be found elsewhere [25]. The fabricated preform was homogeneous porous medium. The fiber volume fraction of the preform was about between 10% and 15%. Compression experiments were performed to test the deformation resistance of the preform under the applied load. The preform deformed relatively small under the pressure of about 1.2 MPa. Therefore, applied pressure was kept between 0 and 1.2 MPa to avoid sever deformation of preform in infiltration experiments.

Table 1
Properties of short carbon fibers.

Item	Value
Fiber type	T300
Fiber diameter (μm)	6–8
Tensile strength (MPa)	3500
Young's modulus (GPa)	230
Elongation (%)	1.5
Density (g/cm^3)	1.76

The chemical compositions and physical properties of AZ91D magnesium alloy are listed in Tables 2 and 3, respectively. The alloys were melted in stainless steel crucible and bubbled up to reduce the oxygen content in liquid alloy with argon flowing through for at least 60 min. Although the reaction between stainless steel and melt magnesium alloy can be happened somewhat, our studies show that this reaction is not serious under the experimental scale. So it is safe. Surface tension and contact angle between carbon fiber and magnesium alloy are 600 mN m^{-1} [26] and 120 °C [27], respectively.

2.2. Experimental procedures

Visualization is frequently used to study the flow nature of fluid in porous preform at macro and micro levels [15,20] which bridges the gap between physical modeling and real flow phenomena. For this purpose, a measuring device for vacuum assistant pressure infiltration monitored by data acquisition system was designed. Its main features were schematically illustrated in Fig. 1. The experimental device was assembled by infiltration systems, pressure control system, temperature control system, vacuum system, and temperature measurement system. The pressure control system can keep the pressure in the crucible precisely from 0 to 1 MPa. Temperature control system was used to melt AZ91D alloy and preheat short carbon fiber preform. The vacuum in the crucible was maintained at 10–15 kPa by the 2XZ-2B vacuum pump. The high-precision K-type thermocouples of 1 mm in diameter were used in the temperature measurement system to obtain the temperature information during infiltration process. All the thermocouples were inserted into the

Table 2
Chemical compositions of AZ91D alloy.

Al	Zn	Mn	Si	Mg
9.1	0.84	0.30	0.04	Bal.

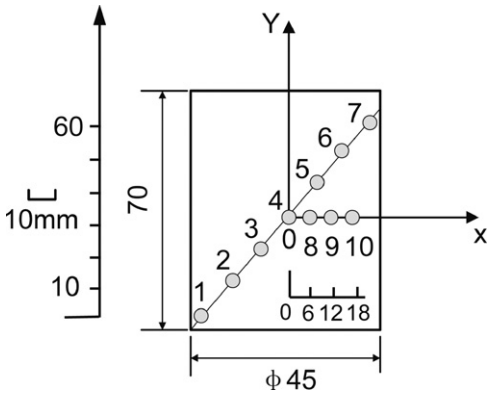

Fig. 2. Thermocouple locations in the preform.

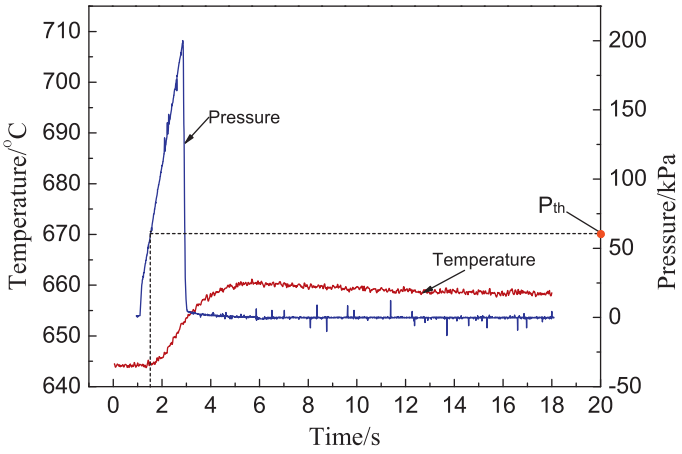

Fig. 4. The pressure–temperature relationship of liquid AZ91D magnesium alloy into 12% carbon perform.

preform, seven from which were in the vertical direction and four from which were in the radial direction. Thermocouples 4, 8, 9 and 10 were used to observe whether the magnesium alloy infiltrated into carbon preform in laminar way. The vertical distance between thermocouples was 10 mm, which can minimize flow disturbance along the vertical direction. The locations of thermocouples were shown in Fig. 2. A multi-function data acquisition card PCI-1710-B and HGWR2061 temperature transmitters were used to segregate, amplify and filter signals of the temperature. During the infiltration experiments, temperature of every thermocouple was recorded at frequency 500 per second.

The dynamic evolution of infiltration front was visualized by analyzing the temperature variation of specific points in the preform during the infiltration process. After assembled, a vacuum of 10 kPa was attained by means of vacuum pump, followed by the introduction of argon up to a pressure of 0.1 MPa to prevent the molten magnesium and carbon preform being oxidized during the melting process. The preform was preheated to an average temperature of 600 °C and AZ91D magnesium alloy was superheated to 800 °C for complete melting. When magnesium alloy ingot was completely melted, the liquid alloy was in equilibrium state in an argon atmosphere. Then, vacuum pump was turned on to exhaust out the argon of the preform through the graphite paper and pressure was raised up to a chosen value at the same time. Under the driving force from the pressure difference, the melting magnesium alloy infiltrates into the carbon fiber preform. By recording the time of temperature changing monitored by the thermocouples placed in the preform, evolution of infiltration front could be determined according to Fig. 3. From the experimental results, it can be seen that the temperature gradient of preform in radial direction was in the range of 20 °C. The effects of radial temperature on the infiltration front were very small. Infiltration was with a relatively plane front and with small perturbation from cooling along the side walls. So the relationship between the infiltration height and infiltration time can be obtained based on the thermocouples from 1 to 7. In Experiments, three different gas pressures were used to infiltrate liquid magnesium into preform, namely 0.4, 0.5 and 0.6 MPa, through which effect of pressure on the infiltration behavior can be investigated.

To measure directly the threshold pressure of AZ91D magnesium alloy infiltrating into carbon preform, an electrical proportional valve was used to control the infiltration pressure linearly from 0 kPa to the setting value. A thermocouple was inserted into the bottom of perform to monitor the time for the infiltration initiating. Threshold pressure can be calculated from the product of determined time and the rate of pressure growth. Fig. 4 shows the recorded pressure–temperature relationship of AZ91D magnesium alloy into 12% carbon preform. In particular, infiltration experiments were performed at preheat temperature 600 °C for preform and the gas pressure was controlled to linearly increase from 0 kPa to 200 kPa in 2 s. It can be seen that when the gas pressure was less than the threshold pressure, liquid magnesium alloy could not infiltrate into the carbon perform. Until the gas pressure was increased to the threshold pressure, the temperature monitored by thermocouple increased suddenly and infiltration began. Although the infiltration process is so fast due to the very high permeability of the carbon preform, the proposed method is still capable of measuring threshold infiltration pressure accurately. In Fig. 4, the threshold infiltration pressure corresponding to the time of a first temperature changing can be found as 54 kPa.

3. Results and discussion

3.1. Infiltration kinetics and permeability

3.1.1. Darcy's law and permeability

Fig. 5 shows the experimental results for the square of the infiltrated height z^2 to infiltration time t at a different constant applied pressure p. The linear relationship between the square of infiltration height and the infiltration time at different infiltration pressure can be obtained which can be satisfactorily described by Darcy's law as shown in Eq. (1) [28].

$$z^2 = \frac{2t}{A} \cdot \Delta p = \frac{2t}{A}(p_a - p_{th}) \quad (1)$$

where t is the infiltration time, p_a is the applied pressure, p_{th} is the threshold pressure for the initiation of infiltration, A can be considered as an intrinsic parameter of the infiltration process comprising

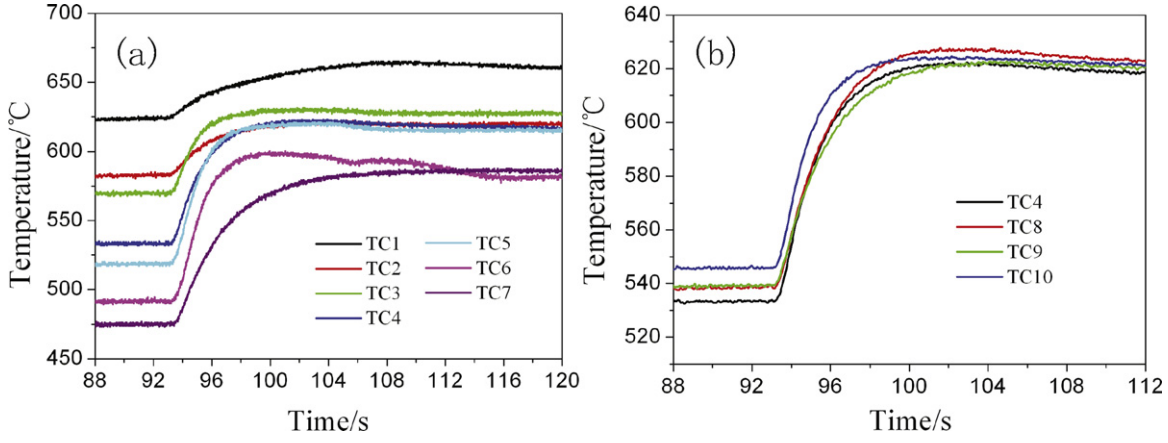

Fig. 3. Temperature variations during the experiment at gas pressure of 0.5 MPa: (a) thermocouple 1–7 and (b) thermocouple 4 and 8–10.

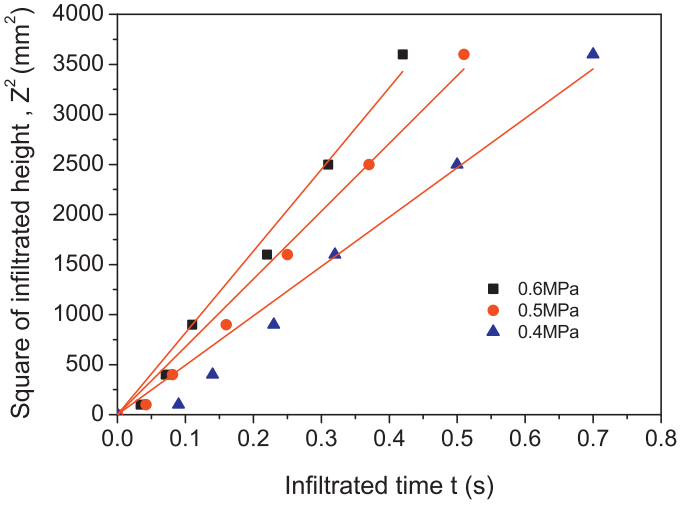

Fig. 5. Square of the infiltrated height z^2 vs the infiltration time for different applied pressures. The fitted straight lines are: $z^2 = 8166t$ for 0.6 MPa, $z^2 = 6772t$ for 0.5 MPa, $z^2 = 4933t$ for 0.4 MPa.

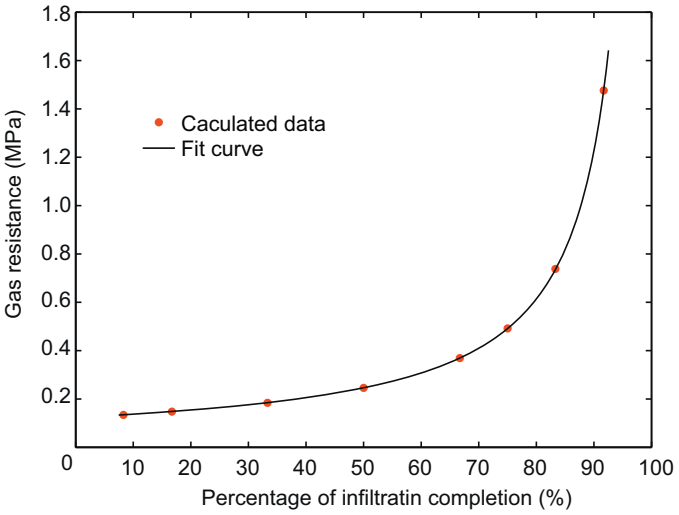

Fig. 6. The relationship between gas resistance and the percentage of infiltration completion during infiltration.

properties from the liquid metal and porous fiber preform, which is given by

$$A = \frac{\mu(1-v_f)}{K} \tag{2}$$

It should be noted that the value of A depends on the viscosity of the liquid alloy, μ, the volume fraction of the fiber preform, v_f, and the permeability K. K is termed the "permeability" of the porous medium, and is a function of the medium's geometry such as the connectivity and dimensions of the pores.

3.1.2. Threshold pressure model

A minimum pressure is required for initiating infiltration when the metal does not wet the preform [29]. Studies on infiltration of particle preform have shown that the threshold pressure can be accurately predicted by use of the capillary law [30]. However, for infiltration of preform made from short fibers, systematic studies have not been reported yet. In addition, the gas anti-pressure was not considered in the analysis of the threshold pressure before.

The threshold pressure [17,23] p_{th} for infiltration of short fiber preform can be obtained as

$$p_{th} = -\frac{2\sigma_{lg}\cos\theta}{r_{eq}} = -\frac{6\lambda\sigma_{lg}\cos\theta v_f}{d_f(1-v_f)} \tag{3}$$

where σ_{lg} is the liquid–vapor surface tension and λ is a geometrical factor introduced to describe deviations from fiber shape and surface roughness. r_e is the equivalent radius and defined as

$$r_{eq} = \frac{n}{2v_f}d_f = \frac{1-v_f}{2v_f}d_f \tag{4}$$

For the C_{sf}/AZ91D composite, the contact angle and the surface tensions were 120° and 600 mN m^{-1}, respectively. Based on the experimental threshold pressure 54 kPa for the preform of the volume fraction of 12%, λ can be determined as $\lambda = 3$. The threshold pressure for the C_{sf}/AZ91D composite by the vacuum infiltration can be expressed as Eq. (5) without a consideration of anti-pressure after introducing λ into Eq. (3).

$$p_{th} = -\frac{2\sigma_{lg}\cos\theta}{r_{eq}} = -\frac{18\sigma_{lg}\cos\theta v_f}{d_f(1-v_f)} \quad (0 \le z \le L) \tag{5}$$

It is noted that the above procedures are based on the ideal vacuum state of the process. However, it is difficult to achieve an ideal vacuum in experiments. The anti-pressure of gas plays an essential role in the infiltration process and especially during the determination of the threshold pressure. The anti-pressure of gas increases dramatically with the increase of the infiltration depth. It is also affected by ambient temperature. Increase or decrease of the temperature will cause related increase or decrease of the anti-pressure. When the infiltration height arises from $\mathbf{z_0}(t=0)$ to $\mathbf{z}$, the volume ratio of gas remaining in the preform is $V_0/V_1 = L/(L-z)$. By the state equation of the ideal gas $PV = nRT$, the gas anti-pressure can be defined as

$$p_g(z) = \frac{p_0 T_Z L}{T_0[L-z]} \quad (0 \le z \le L) \tag{6}$$

where p_0 is the gas pressure at initial time, T_0 is the temperature at initial time, T_z is the gas temperature as the infiltration height is z, and L is the total length of preform.

As seen in Fig. 6, if the residual gas in the preform is not discharged, the anti-pressure generated by gas compression increases rapidly with the infiltration processing. High pressures are needed for the infiltration to occur. It is suggested that gas volumes in preform have a significant effect on the determination of infiltration parameters.

According to the above analysis, the threshold pressure for the infiltration of AZ91D magnesium alloy into the short carbon fiber preform can be determined through Eq. (7) considering the anti-pressure.

$$p_{th} = -\frac{18\sigma_{lg}\cos\theta v_f}{d_f(1-v_f)} + \frac{p_0 T_z}{T_0} \tag{7}$$

3.1.3. Validation and discussion of the threshold pressure model

Experimental measurement of the threshold pressure was carried out to verify the results from Eq. (5) first by use of the preform with volume fraction in the range 10–15%. The facility set-up for the experiment is schematically shown in Fig. 1. The experimental process has been described in Section 2.2. For this purpose, preforms

Table 3
Physical properties of AZ91D.

Item	Value
Kinematic viscosity (Pa s)	0.003 (at 963 K)
Specific heat (J/kg·K)	1014(at 20 °C)
Thermal conductivity (W/m K)	72 (at 20 °C)
Density (g/cm^3)	1.81
Solidus (°C)	470
Liquidus (°C)	595

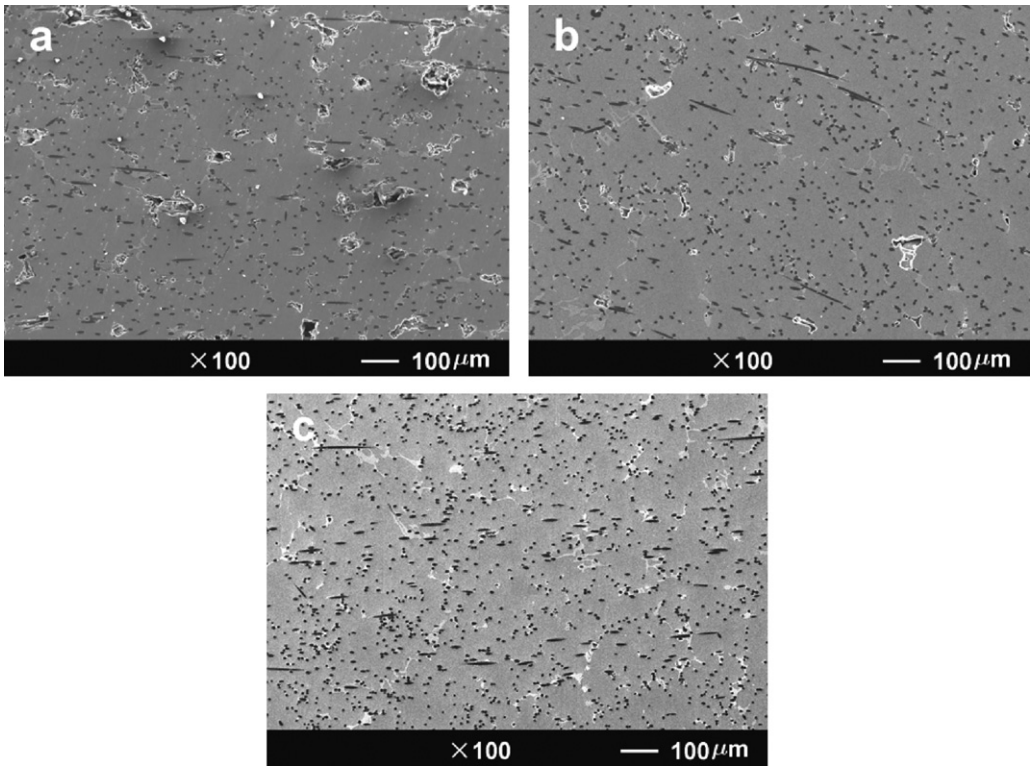

Fig. 7. SEM micrographs of the C_{sf}/AZ91D composites prepared under different infiltration pressures: (a) 0.4 MPa, (b) 0.5 MPa, (c) 0.6 MPa.

with a height of 25 mm and a diameter of 45 mm were prepared by a wet forming process. The experimental result of threshold pressure is 54 kPa when the volume fraction is 12%, while the predictive value is 52.6 kPa calculated by Eq. (5). As shown in Table 4, the maximum deviation between the measuring threshold pressure and that of model prediction is about 4.6%. The main reason of a lot of difference in experimental result and calculated value is the anti-gas pressure of residual gas in preform. In experimental process, the gas is not easy to be exhausted, resulting in the larger anti-gas pressure. So, the experimental results are greater than the calculated values. However, it still can be concluded that the models are capable of predicting the actual infiltration results.

3.2. Effects of infiltration pressure

The melt alloy tends to flow into the largest pores of the preform firstly while the narrowest pores, which require higher pressures to be infiltrated, can only be filled under enough pressure [31]. Therefore pores with different shape and size may be left after the infiltration which cause infiltration defects. For example, at lower pressures, the composite would have a large number of micropores with a size of about 50–100 μm. Fortunately, increasing infiltration pressure can reduce the size and number of pores so that the quality of composite materials was improved, as shown in Fig. 7.

Preform is infiltrated over a specific range of pressures, and there always exists a region of unsaturated metal flow during infiltration, in which the liquid metal only fills a partial preform. On the other hand, according to Darcy's law, the increasing infiltration pressure can increase the depth of infiltration and the speed of molten metal, which helps to reduce heat loss during the infiltration process. So an optimized infiltration pressure must exist to ensure the liquid metal to infiltrate into the preform while maintaining the stability of the fiber preform in experiment. The experiments results showed that composite has no obvious pore defects when the infiltration pressure reaches 0.6 MPa. So the suitable infiltration pressure can be set 0.6 MPa.

Table 4
Threshold pressure for infiltration of AZ91D alloy into short carbon perform with different volume fraction.

Carbon fiber (vol.%)	Exp. p_{th} (kPa)	Cacul. p_{th} (kPa)	Error (%)
10	45	42.9	4.6
12	54	52.6	2.6
15	71	68.1	4

4. Conclusions

1. Isothermal unidirectional infiltration experiments have been carried out with pressurized gas, in which quantitative measurements of infiltration kinetics and threshold infiltration pressure can be realized.
2. Theoretical models have been empirically quantified by the experimental results of short carbon fiber preform infiltrated by melting AZ91D magnesium alloy with different infiltration pressures.
3. The infiltration pressure is slightly underestimated by the model presented here. This is attributed to air-entrapment in the preform during infiltration.

Acknowledgements

The authors are grateful for the financial supports from the National Nature Science Foundation of China (No. 50972121), the fund of the State Key Laboratory of Solidification Processing in NWPU (Nos. SKLSP201103, SKLSP201008), and Science and Technology Innovation Foundation of Northwestern Polytechnical University (No. 2010KJ0202).

References

[1] F.Z. Ren, J.C. Gao, W. Li, M. Zhang, Z. Tan, Carbon 50 (2012) 343.
[2] L.Z. Su, L.H. Qi, J.M. Zhou, H.J. Li, J. Alloys Compd. 509 (2011) 775.
[3] K. Dash, B.C. Ray, D. Chaira, J. Alloys Compd. 516 (2012) 78.
[4] Y.R. Zhu, Y.Y. Chen, G.H. Xu, X.J. Ye, D.N. He, J. Zhong, Mater. Sci. Eng. C 32 (2012) 390.
[5] K.B. Nie, X.J. Wang, L. Xu, K. Wu, X.S. Hu, M.Y. Zheng, J. Alloys Compd. 512 (2012) 355.
[6] A. Mortensen, J.A. Cornie, Metall. Trans. A 18A (1987) 1160.
[7] T.W. Clyne, J.F. Mason, Metall. Trans. A 18A (1987) 1519.
[8] J. Hu, G. Liu, S.W. Tang, J. Alloys Compd. 513 (2012) 61.
[9] J.M. Molina, J. Tian, J. Narciso, E. Louis, J. Mater. Sci. 45 (2010) 2816.
[10] B. Xiong, H. Yu, Z. Xu, Q. Yan, C. Cai, J. Alloys Compd. 509 (2011) L279.
[11] S.S. Hwang, J.H. Han, D.Y. Lee, S.W. Park, J. Alloys Compd. 509 (2011) L336.
[12] L.H. Qi, L.Z. Su, C.X. Jiang, J.M. Zhou, H.J. Li, Mater. Sci. Eng. A 454–455 (2007) 608.
[13] Z.J. Wang, L.H. Qi, J.M. Zhou, F. Yang, Acta. Metall. Sin. 43 (2007) 857.
[14] S. Long, Z. Zhang, H.M. Flower, Acta. Metall. Mater. 42 (1994) 1398.
[15] G. Kaptay, Compos. Sci. Technol. 68 (2008) 228.
[16] J.M. Molina, R.A. Saravanan, R. Arpon, C. Garcia-Cordovilla, E. Louis, J. Narciso, Acta Mater. 50 (2002) 247.
[17] V.J. Michaud, A. Mortensen, Metall. Trans. A 23A (1992) 2263.
[18] V.J. Michaud, L.M. Compton, A. Mortensen, Metall. Mater. Trans. A 25A (1994) 2145.
[19] S. Long, Z. Zhang, H.M. Flower, Acta Metall. Mater. 43 (1995) 3499.
[20] P. Yu, M. Qian, L. Li, G.B. Schaffer, Acta. Mater. 58 (2010) 3790.
[21] H. Tan, K.M. Pillai, Composites A 43 (2012) 1.
[22] L.H. Qi, R. Xu, L.Z. Su, J.M. Zhou, J.T. Guan, Trans. Nonferrous Met. Soc. China 20 (2010) 980.
[23] A. Rodriguez-Guerrero, S.A. Sanchez, J. Narciso, E. Louis, F. Rodriguez-Reinoso, Acta Mater. 54 (2006) 1821.
[24] L.J. Masur, A. Mortensen, J.A. Cornie, M.C. Flemings, Metall. Trans. A 20A (1989) 2549.
[25] H.B. Ouyang, H.J. Li, L.J. Qi, Z.J. Li, T. Fang, J.F. Wei, J. Mater. Sci. 43 (2008) 4618.
[26] L.S. Turng, K.K. Wang, J. Mater. Sci. 26 (1991) 2173.
[27] H. Takuda, H. Fujimoto, N. Hatta, J. Mater. Process. Technol. 80–81 (1998) 513.
[28] C. Garcia-cordovilla, E. Louis, J. Narciso, Acta Mater. 47 (1999) 4451.
[29] A. Rodriguez-Guerrero, J. Narciso, E. Louis, F. Rodriguez-Reinoso, Compos. Sci. Technol. 68 (2008) 75.
[30] J.M. Molina, J. Narciso, E. Louis, Scripta Mater. 62 (2010) 961.
[31] V.J. Michaud, L.M. Comption, A. Mortensen, Metall. Mater. Trans. A 25 (1994) 2145.